

Pharmaceutics, Drug Delivery and Pharmaceutical Technology

D-Optimal Design in the Development of Rheologically Improved *In Situ* Forming Ophthalmic Gel

Iva Krtalić¹, Senka Radošević¹, Anita Hafner², Mario Grassi³, Mirta Nenadić², Biserka Cetina-Čižmek¹, Jelena Filipović-Grčić², Ivan Pepić², Jasmina Lovrić^{2,*}

¹ R&D, PLIVA Croatia Ltd, TEVA Group Member, Prilaz baruna Filipovića 25, 10000 Zagreb, Croatia

² Department of Pharmaceutical Technology, University of Zagreb, Faculty of Pharmacy and Biochemistry, A. Kovačića 1, 10000 Zagreb, Croatia

³ Department of Engineering and Architecture (DIA), University of Trieste, Via Alfonso Valerio 6/A, I 34127 Trieste, Italy

ARTICLE INFO

Accepted 24 January 2018

Keywords:
ophthalmic drug delivery
quality by design (QbD)
chitosan
rheology
gel

ABSTRACT

In situ forming ophthalmic gels need to be fine tuned considering all the biopharmaceutical challenges of the front of the eye in order to increase drug residence time at the application site resulting in its improved bioavailability and efficacy. The aim of this study was to develop *in situ* forming ophthalmic poloxamer P407/poloxamer P188/chitosan gel fine tuned in terms of polymer content, temperature of gelation, and viscosity. Minimizing the total polymer content while retaining the advantageous rheological properties has been achieved by means of D-optimal statistical design. The optimal *in situ* forming gel was selected based on minimal polymer content (P407, P188, and chitosan concentration of 14.2%, 1.7%, and 0.25% w/w, respectively), favorable rheological characteristics, and *in vitro* resistance to tear dilution. The optimal *in situ* forming gel was proved to be robust against entrapment of active pharmaceutical ingredients making it a suitable platform for ophthalmic delivery of active pharmaceutical ingredients with diverse physicochemical properties.

Introduction

The anatomical barriers and the tear fluid dynamics in the precorneal area of the eye have a huge effect on the eye-related drug bioavailability.¹ This problem can be overcome by using *in situ* forming ophthalmic gels prepared from polymers that exhibit reversible phase transitions and pseudoplastic behavior to minimize interference with blinking and avoid foreign body sensation and blurring of vision.²⁻⁴ *In situ* forming ophthalmic gels need to be fine tuned considering all the biopharmaceutical challenges of the front of the eye in order to increase drug residence time at the application site resulting in its improved bioavailability and efficacy.⁵ Such a system should be formulated as drug containing liquid suitable for instillation into the eye that shifts to the gel phase upon exposure to physiological conditions.⁶ The optimal *in situ* forming gel should be characterized by: (1) temperature of gelation (T_{gel}) in physiologically relevant range; (2) pseudoplastic behavior that

allows gel to thin during blinking, making it more comfortable and easier to spread across the eye surface⁷; (3) suitable gel strength to endure the dilution with tears. Moreover, *in vivo* performance of *in situ* forming ophthalmic gels is governed also by drug release and biocompatibility issues.

Poloxamers (Pluronic®), a series of closely related block copolymers of polyethylene oxide and polypropylene oxide, have been investigated as *in situ* forming gels.⁸ At high concentrations of poloxamers, the aqueous solutions exhibit a dramatic change of the viscoelastic moduli and become soft solids or gels. A phase transition from liquid to gel upon reaching physiological temperatures is presently one of the most important phenomena for their applications.⁹ Poloxamer 407 (P407) was mainly studied for ophthalmic delivery, however, concentrated P407 aqueous solutions (>18%, w/w) gel already at the ambient temperature.¹⁰ In that case, *in situ* forming ophthalmic gel has to be stored in refrigerator and applied cold,⁶ and therefore, its instillation to the front of the eye can possibly be irritating and painful.

The use of P407 in mixture with other poloxamers is considered as a strategy to decrease the P407 concentration and to modulate the temperature of gelation and rheological properties of *in situ* forming gel. Among others, poloxamer 188 (P188) was shown to be a good modulator of P407 *in situ* forming gels.¹⁰⁻¹² In previous studies, both poloxamers were used in *in situ* forming ophthalmic

This article contains supplementary material available from the authors by request or via the Internet at <https://doi.org/10.1016/j.xphs.2018.01.019>.

* Correspondence to: Jasmina Lovrić (Telephone: +385 1 63 94 763; Fax: +385 1 46 12 691).

E-mail address: jlovric@pharma.hr (J. Lovrić).

gels at very high total concentration, for example, P407 and P188 in concentration of 21% and 10%,¹⁰ 16% and 14%,¹³ 20% and 11%¹⁴ (w/w), respectively.

The additional improvements in the biopharmaceutical properties of poloxamer ophthalmic gels can be achieved by the presence of different additives in the formulation.¹⁵⁻¹⁹ Chitosan, a biocompatible and biodegradable polycationic polymer, has been demonstrated to increase the mechanical strength and mucoadhesiveness of *in situ* forming ophthalmic gels.¹⁹ In addition, there are other benefits of including chitosan in ophthalmic formulations such as improvement of eye-related permeability due to its paracellular permeation enhancing effects,²⁰ antimicrobial activity,²¹ and corneal wound healing effect.²²

The aim of this study was to develop *in situ* forming ophthalmic poloxamers/chitosan gel fine tuned in terms of polymer content and rheological properties, that is, temperature of gelation, storage modulus, and viscosity. Minimizing the total polymer content while retaining the advantageous rheological properties has been achieved by means of D-optimal statistical design. The selection of the leading candidate for drug formulation development has been based on the ability to keep its rheological properties upon dilution under biorelevant conditions. The robustness of selected mixed system has been evaluated upon entrapment of 4 ophthalmic active pharmaceutical ingredients (APIs).

Materials and Methods

Materials

Poloxamers P407 (Kolliphor P407; EO₉₈PO₆₉EO₉₈; average molecular weight (M_w) 13,498 g/mol) and P188 (Lutrol micro F68; EO₈₀PO₂₇EO₈₀; average M_w 8902 g/mol) were purchased from BASF SE (Ludwigshafen, Germany). More than 90% deacetylated ultrapure PROTASAN™ chitosan salt (Protasan UP CL214; M_w 150,000-400,000 g/mol; viscosity 20-200 mPa × s) (CS) was obtained from NovaMatrix® (Sandvika, Norway). Timolol maleate (TIMO), dexamethasone (DEX), dorzolamide hydrochloride (DORZO) were kindly donated by TEVA Pharmaceutical Industries Ltd. Tobramycin (TOBRA) standard was purchased from the United States Pharmacopeia (Rockville, MD).

Simulated tear fluid (STF), pH 7.4, was prepared by dissolving the following substances in double-distilled water: KCl (1.4 mg/mL), NaCl (6.8 mg/mL), NaHCO₃ (2.2 mg/mL), and CaCl₂ × 2H₂O (0.08 mg/mL).²³ Final step in STF preparation was filtration of solution (Whatman™ membrane filters, 0.2 μm, RC58; GE Healthcare Limited, Buckinghamshire, UK).

Cellulose acetate 0.8 μm membranes for *in vitro* release (IVR) test (CA 0.8) were obtained from Sartorius Stedim Biotech (Göttingen, Germany).

Preparation of In Situ Forming Ophthalmic Gels

In situ forming ophthalmic gels were prepared by slightly modified cold method.²⁴ Briefly, appropriate amounts of all materials were weighed in a glass bottle and defined amount of previously refrigerated water for injection (WFI; PLIVA Croatia Ltd.) was added. Samples were stirred (speed 400-600 rpm) in an ice bath until clear solution was obtained. In case when CS was used in mixed systems, after ice bath, additional means of ultrasound at 20°C-25°C (Bandelin Sonorex digital 10P; BANDELIN electronic GmbH & Co. KG, Berlin, Germany) was applied to aid its dissolution. All prepared systems had an ophthalmically acceptable osmolality, which was achieved by the addition of appropriate amounts of NaCl to the solution. Osmolality was determined by the freezing point depression method (Advanced® 3D3 Single-Sample Osmometer; Advanced Instruments Inc., Norwood, MA). For CS-free solutions, it

was in the range of 295.4-301.8 mOsm/kg, whereas for CS-containing solutions, it was in the range of 310.4-332.0 mOsm/kg. pH was measured using PHM240 pH/Ion Meter (Radiometer Analytical SAS, Villeurbanne, France) and was in the range of 5.8 for CS-containing solutions to 6.5 for CS-free solutions. The transparency of *in situ* forming ophthalmic gels was determined by measuring the refractive index (RE40 Refractometer; Mettler-Toledo, LLC, Columbus, OH). Refractive index of all systems was in the ophthalmically suitable range for eye drops (i.e., not greater than 1.476²⁵).

Out of 4 APIs, 6 API-loaded *in situ* forming ophthalmic gels were prepared, namely mixed P407/P188/CS system containing: 2% (w/w) DORZO, 0.5% (w/w) TIMO, 2% (w/w) DORZO, and 0.5% (w/w) TIMO, 0.1% (w/w) DEX, 0.3% (w/w) TOBRA, 0.05% (w/w) DEX and 0.3% (w/w) TOBRA. *In situ* forming ophthalmic gels containing TIMO, DEX, and DORZO were prepared in same way as API-free systems. For preparation of systems containing TOBRA, API was first dissolved in defined aliquot of WFI and then mixed with P407/P188/CS solution. pH was adjusted to 5.8 since addition of TOBRA increased pH of the solution. All *in situ* forming ophthalmic gels were isotonized taking into account NaCl equivalent for each API.

Measurement of Temperature of Gelation and Complex Viscosity

The temperature sweep test was performed to determine the T_{gel}, the temperature dependence of complex viscosity (η*) and the temperature dependence of storage (G') and loss modulus (G'').^{17,26} The rheological measurement was performed using Rheometer Anton Paar Physica MCR 301 (Anton Paar GmbH, Graz, Austria) with parallel plate (PP50) measuring system equipped with H-PTD 200 Truly Peltier temperature-controlled hood (U.S. Patent 6,571,610) connected to circulating water bath (JULABO GmbH, Seelbach, Germany). Samples were equilibrated at 5°C for 5 min. Angular frequency and strain applied were fixed at 1 s⁻¹ and 1%, respectively, whereas gap was d = 0.5 mm. Data were calculated by Rheoplus™ software (Anton Paar).

G', G'', and η* were recorded in the temperature range of 5°C-85°C with a rate of 10°C/min. T_{gel} is defined as the temperature point at which intersection of G'' and G' curves occurs.^{17,27} All measurements were done in triplicate.

Design of Experiments

Quality by Design principles were employed to optimize formulation parameters and evaluate their impact on T_{gel}, G', and η*. Statistical software JMP®, version 12.0.1, (SAS Institute Inc., Cary, NC) was used to set of experimental design, establish the mathematical models, and analyze the collected data. Designs were generated within the class of optimal designs, and D-optimality criterion was selected based on the particularities of the experimental situation.

The independent variables were the concentration of P407, P188, and CS, whereas dependent variables were T_{gel}, G', and η* obtained from temperature sweep test. Sequential approach to experimentation was applied through screening, refining, and optimizing designs (Table 1). Data set was initiated with the results of preliminary screening, consisting of 5 samples, which contained only P407. For the subsequent design of experiment (refining), a new factor was added in order to explore influence of concentration levels of CS on the responses and include it into the model. Finally, to evaluate the error of mixed system preparation and measurement, 3 replicated samples were added.

Data were checked for the basic assumptions needed for the statistical test. Normality of the data was tested with Kolmogorov test. Log-transformed response variables G' and η* were fitted

Table 1
Sample Sequence From Design of Experiment (DoE) and Corresponding Experimental Temperature of Gelation (T_{gel}), Complex Viscosity (η^*), Storage Modulus (G'), and Damping Factor

DoE	Sample ^a	P407	P188	CS	T_{gel}	η^*	$\log\eta^*$	G'		Damping Factor ($\tan\delta$)	Form	
		(%, w/w)	(%, w/w)	(%, w/w)	(°C)	(Pa × s)	(Pa)	$\log G'$				
Preliminary screening	1 ^o	11.4			33.4	0.05	-1.34	3.56	0.55	0.825	Gel	
	2 ^o	13.8			24.4	19.5	1.29	119	2.08	0.259	Gel	
	3 ^o	15.2			24.3	702	2.85	4320	3.64	0.206	Gel	
	4 ^o	16.9			20.7	1520	3.18	9360	3.97	0.197	Gel	
	5 ^o	19.3			15.1	2430	3.39	15,200	4.18	0.101	Gel	
Screening	6 [•]	11.32	0.87		31.6	0.44	-0.36	2.45	0.39	0.494	Gel	
	7 [•]	19.1	0.8		15.1	2370	3.37	14,700	4.17	0.142	Gel	
	8 [•]	15.8	0.84		22.5	277	2.44	1660	3.22	0.315	Gel	
	9 [•]	14.12	4.01		29.8	2.17	0.34	13.20	1.12	0.248	Gel	
	10 [•]	14.61	4.24		33.4	1.21	0.08	7.01	0.85	0.413	Gel	
	11 [•]	18.39	4.64		22.5	131	2.12	794	2.90	0.271	Gel	
	12 [•]	10.59	7.4		49.4	0.02	-1.68	n.d.	n.d.	1E+30	Solution	
	13 [•]	15.49	7.66		35.1	0.48	-0.32	4.30	0.63	0.685	Gel	
	14 [■]	16.4	0.85	0.08	23.8	169	2.23	975	2.99	0.425	Gel	
Refining step (addition of CS)	15 [■]	10.93	4.2	0.08	52.5	0.02	-1.61	0.0156	-1.81	9.46	Solution	
	16 [■]	15.92	3.97	0.08	31.1	7.77	0.89	46.4	1.67	0.327	Gel	
	17 [■]	13.61	2.51	0.66	33.5	0.54	-0.27	9.17	0.96	0.748	Gel	
	18 [■]	11.16	0.95	1.29	54.8	0.4	-0.4	0.27	-0.56	9.09	Solution	
	19 [■]	16.2	0.92	1.22	26.3	26.2	1.42	229	2.36	0.201	Gel	
	20 [■]	10.8	4.18	1.25	47.7	0.49	-0.31	0.93	-0.03	3.14	Solution	
	21 [■]	15.7	3.96	1.18	33.5	3.32	0.52	35.6	1.55	0.46	Gel	
	22 [■]	11.31	0.89	0.10	38.2	0.04	-1.4	n.d.	n.d.	2.37	Solution	
	Replicate step	23 (14) ^o	16.4	0.84	0.09	23.9	1245	3.1	7270	3.86	0.2745	Gel
		24 (15) ^o	10.93	4.21	0.09	52.4	0.02	-1.63	0.03	-1.53	12.4	Solution
25 (16) ^o		15.88	3.97	0.08	31.1	2.36	0.37	21.20	1.33	0.2935	Gel	

^a ^o-preliminary screening, [•]-screening, [■]-screening with addition of CS, ^o-optimization step; n.d., not determined.

using a regression model. Logarithmic transformation was found as optimal within Box-Cox power transformation for the responses G' and η^* so the usual regression assumptions of normality and homogeneity of variance were more closely satisfied.

Multiple regression and ANOVAs were used to evaluate experimental results (JMP® version 12.0.1). Factorial models were set to determine all main effects and interactions for the factors of interest, that is, concentrations of P407, P188, and CS. Significance of the regression models was assessed with ANOVA. Level of significance for all tests was $\alpha = 0.05$. Factor Profiling platform (JMP®) was utilized to explore and visualize estimated models, for example, to explore the shape of the response surface, find optimum settings of the factors, and simulate response data.

To validate the models, the experimental values of T_{gel} , G' , and η^* of 4 optimal mixed P407/P188/CS systems were statistically compared with their predicted responses.

Strain and Frequency Sweep Testing

The viscoelastic behavior of *in situ* forming ophthalmic gels was investigated by strain sweep and frequency sweep test using the rheometer system with cone-and-plate (CP50) geometry with 1° incline. Gap in the measuring configuration was $d = 0.05$ mm. For strain sweep analysis, the angular frequency was set at 62.8 rad/s, and the strain was varied from 0.001% to 1000%. The linear viscoelastic (LVE) range at 35°C was identified as the region in which the moduli are independent of the strain. For frequency sweep analyses, strain was set at 1%, which was in the LVE range, whereas the angular frequencies were in the range of 0.628-199 rad/s.

Gelation time was determined as the time point at which intersection of the curves of measured G'' and G' occurred.²⁷ The samples were placed at rheometer plate preheated at 35°C. Strain (1%) was constantly in LVE range, whereas applied frequency was 1 Hz throughout the test.

The evaluation of *in situ* forming ophthalmic gel under biorelevant conditions was performed by sample dilution with STF

(40:7). The STF diluted samples were submitted to strain and frequency sweep analysis at 35°C.

In Vitro Release Study

IVR testing was performed using the Vision Microette (Hanson, Chatsworth, CA), a commercial Franz diffusion cell apparatus equipped with 6 static vertical diffusion cell with 12 mL volume and 15 mm orifice (providing area for release of 1.767 cm²), an AutoFill sample collector and circulating water bath. Donor part of vertical cell consisted of open cell top with cap which is suitable for retaining less viscous liquids. Temperature was maintained at 35°C, and stirring speed of 400 rpm assured homogenized sample in the receptor medium (STF). Sink conditions were assured. An aliquot of 2.5 mL of sample was placed on the CA 0.8 membranes in donor compartment. Suitability of CA 0.8 membranes (low drug adsorption and low diffusion resistance) was demonstrated in the membrane selection study (data not shown).

IVR testing of *in situ* formulations was performed during 24 h. One milliliter of samples was collected automatically at pre-determined time intervals. System's rinsing volume was set at 1.5 mL to assure no carryover of an API prior each sampling point. Quantification of TIMO was done by ultraperformance liquid chromatography as detailed in the [Supplementary Materials and Methods](#).

In Vitro Biocompatibility Study

The biocompatibility was assayed using corneal epithelial models based on the immortalized human corneal epithelial cell line (HCE-T) (RIKEN Cell Bank, Tsukuba, Japan). The cultivation of HCE-T cell-based models was performed as detailed in the [Supplementary Materials and Methods](#). The mixed P407/P188/CS system was applied directly onto cell-based models. After the 30-min treatment at 37°C, treated models were incubated at the room temperature for 5 min to induce formulation gel-sol

transition. The cell surface was rinsed with Hank's balanced salt solution and exposed to air-liquid interface for the following 24 h. The cell viability was assessed by MTT (3-[4,5-dimethylthiazol-2-yl]-2,5-diphenyl tetrazolium bromide) test according to the protocol by Pauly et al.²⁸ as detailed in the [Supplementary Materials and Methods](#).

Results and Discussion

In Situ Forming Ophthalmic Gel Optimization Using a Design of Experiment

The aim of the employed Quality by Design approach was to determine the minimal total concentrations of P407, P188, and CS that would yield an *in situ* forming ophthalmic gel with the potential to ensure the defined formulation characteristics. For the establishment of the mathematical model, it was necessary to generate the data of T_{gel} , G' , and η^* of the sample based on the independent variables (Table 1). In the screening step of the applied sequential approach, influence of concentration levels of 2 factors (independent variables; P407 and P188 concentration) on T_{gel} , G' , and η^* (dependent variables) was tested. Based on the particular experimental conditions, a custom D-optimal design was applied to provide estimates for the effect testing with smallest standard errors, as it maximizes the information in the selected set of experimental runs with respect to a model stated.²⁹ Two center points were included in the experimental runs to allow the testing for nonlinear factor effects and estimation of the pure experimental error and to increase the power of the experiment. A total of 8 experimental runs were generated for the evaluation of the main effects and possible interactions. Accordingly, 8 samples, varying in concentrations of P407 (10.59%-19.1%, w/w) and P188 (0.8%-7.66%, w/w), were prepared, and their T_{gel} , G' , and η^* were determined (Table 1). Collected data were analyzed, and significant cause-and-effect relationship was identified. Data set was expanded with the results of preliminary screening, consisting of 5 samples, which contain only P407 (11.4%-19.3%, w/w).

In the subsequent, refining step, CS concentration was added as an additional independent variable. Concentration ranges of factors P407 and P188 were selected based on the result obtained in screening step, and CS concentration was evaluated in the range of 0.08%-1.29% (w/w) based on the literature data.^{19,30} D-optimal statistical design with 1 center point was applied. Nine experimental runs were required for analyzing the main effects and all second-level interactions. Additionally, to evaluate error of mixed P407/P188/CS system preparation and measurement, 3 replicated runs were added to the experimental sequence (replicate step). Based on this approach, 3 mathematical models were established, that is, T_{gel} , G' , and η^* models, as the prerequisite for the optimization of *in situ* forming P407/P188/CS ophthalmic gel.

The Model of Temperature of Gelation

Within the established T_{gel} model, the response of interest is represented by following regression equation:

$$T_{gel} = 35.46 - 13.84 \times \overline{P407} + 6.70 \times \overline{P188} + 2.74 \times \overline{CS} + 7.07 \times \overline{P407} \times \overline{P188} + 9.16 \times \overline{P407} \times \overline{P188} \times \overline{CS} \quad (1)$$

where factors denoted as overlined represent centered factors, that is reduced by mean value and divided by the half of the factor

range. The obtained coefficient of determination between the experimental and predicted values of T_{gel} was $R^2 = 0.93$ (Fig. S1a).

Statistical analysis of the collected data revealed significant effects of P407, P188, and CS concentrations on the T_{gel} ($p < 0.05$). The concentration effect impacts T_{gel} in following order: P407 (coefficient = -13.84) > P188 (coefficient = 6.70) > CS (coefficient = 2.74). The negative value of the coefficient indicates an inverse relationship between the factor (concentration) and the response (T_{gel}), showing that increase of the P407 concentration will result in a decrease of T_{gel} . The positive value of the coefficient observed for P188 indicates that increasing the concentration of P188 shifts T_{gel} to higher values, as already reported in the literature.^{11,14} Similar to P188, but to a lesser extent, the increase in CS concentration increases T_{gel} . Evidently, CS affects the onset of gelling, but it does not interfere with the formation of *in situ* gel, thus, making it a suitable additive in this mixed poloxamer system. In the similar concentration range, CS was already shown not to induce marked changes in the T_{gel} of poloxamer systems.¹⁹

Significant higher order terms include the interaction between P407 and P188 (coefficient = 7.07) and the interaction among P407, P188, and CS (coefficient = 9.16). These interactions, shown as response surface and contour plots (Figs. 1a-1c), indicate that one factor may vary depending on the level of the other factor. P407 and P188 interaction profile suggests that the impact of P407 on the T_{gel} decrease is more pronounced at the lower level of P188 (Fig. S1b). At the other side, higher level of P407 assures more pronounced effect of P188 on the T_{gel} increase. Curvatures shown on the Figure 1a indicate that this relation is not linear. These interactions reveal the complexity of interplay of the components in the measured mixed systems. The complexity of interplay is highly related to the concentration of P188 in the system as suggested by Zhang et al.¹¹ who revealed the formation of 2 distinct populations of micelles in mixed P407/P188 systems. They suggested that P188 micellization was responsible for the T_{gel} increase.

Models of Rheological Properties: Complex Viscosity and Storage Modulus

Critical attribute that determines the dosing accuracy, retention time, and drug release from *in situ* forming ophthalmic gels is formulation rheological behavior. The systems with fine-tuned rheological properties would withstand the high shear rates and tear dilution thus preventing the drainage of an API from the site of the absorption.⁴

The Model of Complex Viscosity

We investigated and mathematically described the influence of different P407, P188, and CS concentration levels on the measured η^* at 35°C and angular frequency of 1 s^{-1} . Before the statistical analysis, η^* data were checked for normality. Kolmogorov test confirmed that data follow the log-normal distribution. Thus, log transformation was applied on the measured η^* data.

In this mathematical approach, the response of interest [$\log(\eta^*)$] is represented by following regression equation:

$$\log(\eta^*) = -0.37 + 1.53 \times \overline{P407} - 1.60 \times \overline{P188} - 0.55 \times \overline{P407} \times \overline{P188} - 0.76 \times \overline{P407} \times \overline{CS} + 0.70 \times \overline{CS} \times \overline{CS} + 1.56 \times \overline{P407} \times \overline{P407} \times \overline{P188} \quad (2)$$

Developed η^* model shows good fit between experimental and predicted logarithmic values of η^* with resulting coefficient of determination $R^2 = 0.97$ (Fig. S2a).

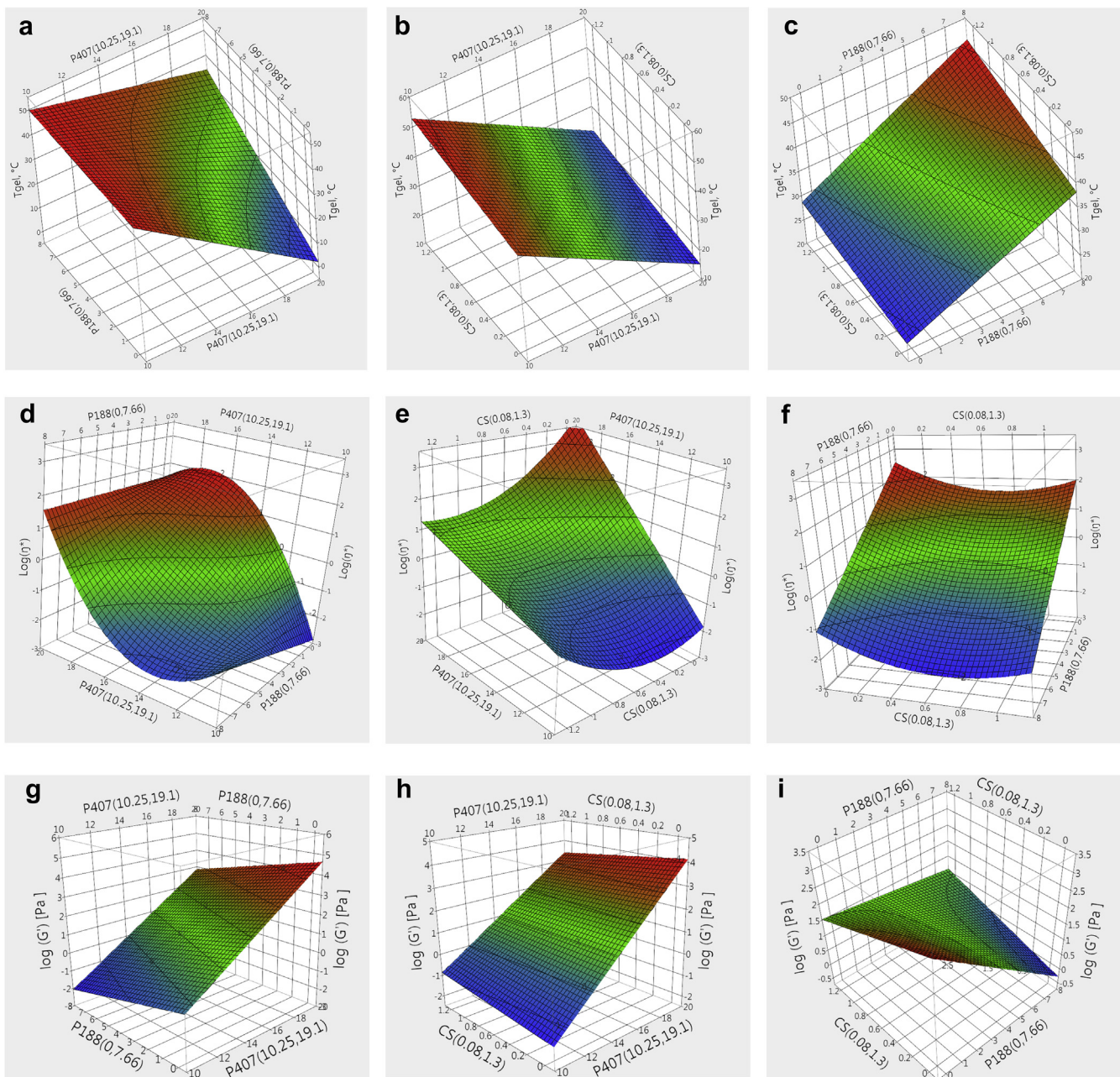


Figure 1. Response surface of the effects of the concentration of P407, P188, and CS on the T_{gel} (a-c), $\log_{10}(\eta^*)$ (d-f), and $\log_{10}(G')$ (g-i). (a) Effect of concentration of P407 and P188 on T_{gel} . (b) Effect of concentration of P407 and CS on T_{gel} . (c) Effect of concentration of P188 and CS on T_{gel} . (d) Effect of concentration of P407 and P188 on $\log_{10}(\eta^*)$. (e) Effect of concentration of P407 and CS on $\log_{10}(\eta^*)$. (f) Effect of concentration of P188 and CS on $\log_{10}(\eta^*)$. (g) Effect of concentration of P407 and P188 on $\log_{10}(G')$. (h) Effect of concentration of P407 and CS on $\log_{10}(G')$. (i) Effect of concentration of P188 and CS on $\log_{10}(G')$.

Statistical analysis of the collected data revealed significant effects of P188 and P407 concentrations on $\log(\eta^*)$ ($p < 0.05$). The increase of P188 concentration results in the decrease of $\log(\eta^*)$ as revealed by its negative coefficient (coefficient = -1.60). On the contrary, the increase of P407 concentration results in the increase of $\log(\eta^*)$ (coefficient = 1.53). The complexity of interactions is noticed on the response surface and contour plots of P407 and P188 (Fig. 1d) and P407 and CS (Fig. 1e), whereas less complex relationship is noticed for P188 and CS on the response (Fig. 1f; which is in agreement with the linear lines on Fig. S2b). The model indicated 2 interactions with negative effect on the response. Namely, these were interaction between P407 and CS (coefficient = -0.76) as well as between P407 and P188 (coefficient = -0.55). Concomitantly,

2 higher order terms were found with the positive effect on the response, namely the interaction among P407, P407, and P188 (coefficient = 1.56), and CS (coefficient = 0.70). At higher level of P188, the effect of P407 on increase of $\log(\eta^*)$ is less pronounced (Fig. S2b). In contrary, the omission of P188 from the system results in faster increase of $\log(\eta^*)$ when increasing P407 concentration. CS and P407 interaction profile suggests that the impact of P407 on the $\log(\eta^*)$ increase is more pronounced at the lower level of CS (Fig. S2b). As it can be seen by comparing the response surface and contour plot images of the T_{gel} model and $\log(\eta^*)$ model (Figs. 1a-1c and 1d-f), higher degree of complexity, that is curvatures, was found in the $\log(\eta^*)$ model. This indicated the absence of linear relationship between the concentrations of 3 tested polymers to a response.

The Model of Storage Modulus

As for the $\log(\eta^*)$, influence of different independent variables (P407, P188, and CS concentration levels) on the measured response G' at 35°C and angular frequency of 1 s^{-1} was tested and mathematically described. Again, Kolmogorov test confirmed that data follow the log-normal distribution; therefore, log transformation was applied on the measured G' data.

$\log(G')$ is described by following regression equation:

$$\log(G') = 1.13 + 2.16 \times \overline{P407} - 0.77 \times \overline{P188} - 0.26 \times \overline{P407} \times \overline{CS} + 0.56 \overline{P188} \times \overline{CS} \quad (3)$$

Developed $\log(G')$ model exhibits suitable fit between experimental and predicted logarithmic values of G' with resulting coefficient of determination $R^2 = 0.93$ (Fig. S3a).

Statistical analysis of the acquired data revealed significant effects of P407 and P188 concentrations on $\log(G')$ ($p < 0.05$), with P407 concentration having stronger effect on the response. As expected, similar to the model for $\log(\eta^*)$, the increase of P188 concentration results in the decrease of $\log(G')$ due to its negative coefficient (coefficient = -0.76). On the contrary, the increase of P407 concentration results in the increase of $\log(G')$ (coefficient = 2.16). As seen on the Figures 1g and 1h, relation between P407 and P188 and P407 and CS on the response in model appears to be relatively simple. More complex relation of P188 and CS on the $\log(G')$ was found to have statistically significant interaction with positive effect on the dependent variable (coefficient = 0.56) (Fig. 1i).

The increase of P188 at lower level of CS results in decrease of $\log(G')$, whereas this effect is not observed when CS is at highest level (1.3%, w/w). The increase in CS at low level of P188 lowers the response of interest. However, this effect is opposite at higher level of P188 (7.66%, w/w).

Another interaction included in the model, but with no statistical significance, was interaction between P407 and CS, having a negative impact on the response (coefficient = -0.26). Same interaction with significant negative effect was noticed in the model for $\log(\eta^*)$.

Selection of Rheologically Improved In Situ Forming Ophthalmic Gel

T_{gel} of innovative ophthalmic *in situ* forming gels is the most critical parameter related to efficacy and safety as well as patient compliance since it influences the accuracy of dosing, (dis)comfort associated with the instillation, and residence time at the eye surface. Namely, if the system gels at room temperature, dosing would be hindered. Storage at low temperature would diminish this problem; however, the instillation of cold formulation can possibly be irritating and painful. Therefore, the optimal T_{gel} *in situ* forming ophthalmic gel should be between 25°C, the average ambient temperature, and 35°C, the eye surface temperature.¹⁹ In our study, the optimal range of T_{gel} was set to 28°C-32°C.

Viscosity is one of the key attributes for innovative ophthalmic *in situ* forming gels defining the residence time at the eye surface and drug release profile. The optimal range of viscosity is much more difficult to select in relation to T_{gel} . A wide range of viscosities reported for poloxamer-based *in situ* forming ophthalmic gels have suitable *in vivo* response.^{6,13,19} Therefore, we characterized the commercially available *in situ* forming ophthalmic gels with rotational test with controlled shear rate (Supplementary Materials) to enable the recognition of leading candidates. Oscillatory tests of selected leading candidates revealed the lower limit for η^* (at 35°C and 1 s^{-1}) at $1.2 \text{ Pa} \times \text{s}$.

Table 2 Selected Mixed P407/P188/CS Systems, Corresponding Experimental and Predicted Temperature of Gelation (T_{gel}), Complex Viscosity (η^*), Storage Modulus (G'), and Damping Factor (Tan δ)

Sample	P407 (% w/w)	P188 (% w/w)	CS (% w/w)	Exp. T_{gel} (°C)	Pred. T_{gel} (°C)	T_{gel} Recovery (%)	Exp. $\log(\eta^*)^a$	Pred. $\log(\eta^*)^a$	$\log(\eta^*)$ Recovery (%)	Exp. $\log(G')^a$	Pred. $\log(G')^a$	$\log(G')$ Recovery (%)	Damping Factor (Tan δ)
PL1	14.2	1.7	0.25	31.10 ± 0.01	31.27 (29.72-32.82)	99.5	0.32 ± 0.06	0.62 (0.28-0.96)	52.4	1.15 ± 0.17	1.53 (1.29-1.78)	76.6	0.29 ± 0.03
PL2	15.0	2.0	0.5	26.30 ± 0.01	28.87 (27.00-30.74)	109.77	0.81 ± 0.06	0.60 (0.06-1.14)	73.8	1.60 ± 0.06	1.75 (1.48-2.02)	91.5	0.21 ± 0.00
PL3	14.2	1.7	1.01	29.90 ± 1.7	35.30 (32.45-38.15)	118.06	0.66 ± 0.02	0.53 (0.09-0.97)	80.2	1.44 ± 0.09	1.18 (0.74-1.62)	122.4	0.26 ± 0.01
PL4	14.2	1.7	0.5	28.70 ± 0.01	32.60 (30.90-34.30)	113.59	0.61 ± 0.09	0.30 (-0.23 to 0.83)	48.9	1.40 ± 0.02	1.42 (1.14-1.70)	98.5	0.23 ± 0.01

Exp., experimental, presented as mean ± SD.

Pred., predicted, presented as mean; values in brackets represent lower and upper limits of 95% CI.

^a η^* (Pa × s) and G' (Pa) at 35°C determined by temperature sweep test (angular frequency and strain were 1 s^{-1} and 1%, respectively).

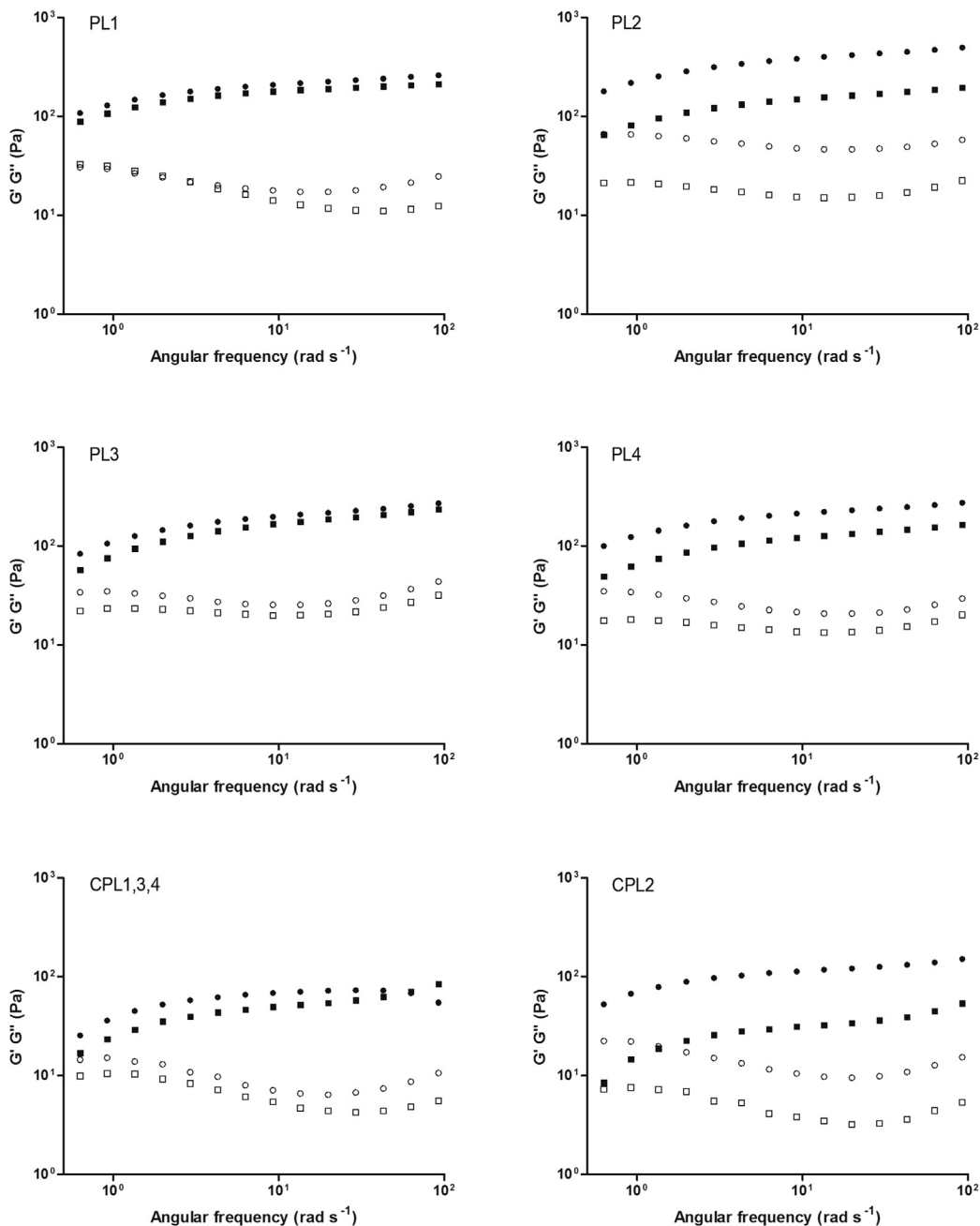


Figure 2. Rheological properties of selected mixed P407/P188/CS systems (PL1, PL2, PL3, and PL4) and respective controls under biorelevant conditions. Frequency sweeps analysis before (circles) and after (squares) dilution with simulated tear fluid (STF) 40:7 at 35°C. G' filled symbols, G'' empty symbols. Control sample for PL1, PL3, and PL4 is labeled CPL1, CPL3, CPL4; control sample for PL2 is labeled CPL2.

G' is a measure of the deformation energy stored by the sample during the shear process. After the load is removed, this energy is completely available, now acting as the driving force for the reformation process which will compensate partially or completely the previously obtained deformation of the structure. G' presents the elastic behavior of a sample, and it assures adequate gel stability. As minimal G' values for gel structures are around 5 Pa,²⁷ this value was set as minimal value for this dependent variable.

Considering the optimal T_{gel} , G' and η^* suggested by corresponding models, 4 mixed P407/P188/CS systems were selected (Table 2). The additional criterion of the selection was the lowest possible total polymer content in *in situ* forming ophthalmic gel. To validate the data obtained by the models, mixed P407/P188/CS

systems were prepared. T_{gel} , G' , and η^* were determined by temperature sweep test and compared with predicted values (Table 2).

High coefficient of determination ($R^2 = 0.93$) and the overall recovery of experimental to predicted T_{gel} ($110.23 \pm 0.08\%$; relative standard deviation [RSD] = 7.02%) confirmed the suitability of T_{gel} model. Similar agreement was found for $\log(G')$ model ($R^2 = 0.93$) with the average recovery of experimental to predicted T_{gel} of $97.25 \pm 19.07\%$, having slightly higher variability (RSD = 19.61%). In case of $\log(\eta^*)$ model, even better coefficient of determination ($R^2 = 0.97$) was observed, and despite the lower overall recovery of experimental to predicted $\log(\eta^*)$ ($63.83 \pm 0.16\%$; RSD = 24.3%), the developed model enabled the development of mixed P407/P188/CS system with targeted viscosity ($>1.2 \text{ Pa} \times \text{s}$). The higher variability

Table 3
Effect of Active Pharmaceutical Ingredients on Temperature of Gelation (T_{gel}) and Complex Viscosity (η^*)

Variable	Before Dilution With STF		After Dilution With STF	
	T_{gel} (°C)	η^* (Pa × s) ^a	T_{gel} (°C)	η^* (Pa × s) ^a
PL1–DORZO	27.50 ± 1.70	7.88 ± 1.18	33.50 ± 0.01	0.67 ± 0.06
PL1–TIMO	26.30 ± 0.01	4.90 ± 0.54	29.90 ± 1.20	2.44 ± 1.50
PL1–DORZO/TIMO	28.70 ± 0.02	4.82 ± 1.07	32.90 ± 0.80	0.64 ± 0.10
PL1–TOBRA	30.30 ± 1.40	1.52 ± 0.66	31.10 ± 0.01	0.52 ± 0.10
PL1–DEX	22.60 ± 1.70	6.11 ± 0.70	28.70 ± 0.01	1.56 ± 1.16
PL1–DEX/TOBRA	23.65 ± 3.18	6.88 ± 1.59	31.15 ± 0.07	0.639 ± 0.21
PL1	31.10 ± 1.40	2.10 ± 0.74	33.50 ± 0.70	0.37 ± 0.15

Values are mean ± SD ($n = 3$).

^a η^* at 35°C determined by temperature sweep test (angular frequency and strain were 1 s^{-1} and 1%, respectively).

of this model could be related to the heating rate-dependent kinetics of gel formation. Mixed P407/P188 systems exhibit very complex rheological behavior with internal relaxations and slow reorganizations taking place in the temperature range preceding or following the T_{gel} .¹¹ However, the fast temperature change is the one expected *in vivo*.

In Depth Rheological Characterization of In Situ Forming Ophthalmic Gel

With the aim of in depth rheological characterization, selected mixed P407/P188/CS systems were subjected to frequency sweep analysis. Strain sweep analysis was carried out to determine the limit of LVE range, that is, the range where stress is directly proportional to strain.

Frequency sweep analysis gives an insight on the behavior of G' , G'' , and η^* as a function of angular frequency. The frequency sweep measurements for all 4 mixed P407/P188/CS systems indicated that G' was higher than G'' revealing suitable gel stability (Fig. 2). Moreover, the presented rheological profile suggests the existence of soft gels known to be formed at moderate poloxamer concentration.³¹ This phenomenon has been ascribed to the weak attraction of spherical micelles as the solvent becomes poorer on heating.

To determine the influence of CS on the gel mechanical strength, frequency sweep analysis was carried out also for the respective control systems without CS (Fig. 2). As expected, the presence of CS in mixed systems resulted in higher G' and G'' values indicating increased gel mechanical strength. It was already suggested that the elastic characteristic of the system increased owing to an effect on microscopic diffusion within gel structure which facilitated the accommodation of unbound water and consequently micelle packaging.¹⁹

Mixed systems were further characterized under biorelevant conditions, that is, diluted with STF at the ratio of 40:7 mimicking their mixing with tear fluid after instillation.¹⁰ Despite the dilution, mixed systems retained their ability to form gel at temperature lower than 35°C (i.e., the sample PL2 formed gel at 28.7°C, whereas PL1, PL3, and PL4 formed gel at 33.5°C). The observed increase in

Table 4
Samples Tested in the IVR Study

Sample	Description/Composition	T_{gel} /°C	η^* (Pa × s)
PL1	14.2% P407, 1.7%P188, 0.25% CS, 0.2% TIMO (w/w)	31.1 ± 2.0	1.2 ± 0.3
C1	14.2% P407, 0.25% CS, 0.2% TIMO (w/w)	26.9 ± 2.2	4.12 ± 1.2
C2	11.4% P407, 0.2% TIMO (w/w)	31.1 ± 1.7	0.097 ± 0.07
TIMO solution	TIMO solution in STF, 2.5 mg/mL	n/a	n.m.

η^* at 35°C determined by temperature sweep test (angular frequency and strain were 1 s^{-1} and 1%, respectively).

n/a, not applicable; n.m., not measured.

T_{gel} relative to undiluted systems (Table 2) can be related to both the decrease in the total concentration of polymers and the modification of the physicochemical properties of the hydrogels in the presence of STF electrolytes.^{19,32}

The dilution of all mixed systems with STF resulted in no change in G' to G'' ratio or their overall profile (Fig. 2). Furthermore, there was no significant change in the absolute values of G' and G'' in case of samples prepared with the same poloxamer concentration and different CS concentration (Fig. 2; PL1, PL3, and PL4). On the contrary, comparing the mixed system PL2 (P407/P188/CS 15.0/2.0/0.5%, w/w) with PL4 (P407/P188/CS 14.2/1.7/0.5%, w/w), it may be observed that the small increase in poloxamer concentration influenced the resistance to dilution.

The decrease of η^* values with the increase of angular frequency arguments suitable pseudoplastic behavior of *in situ* forming ophthalmic gels. The viscosity profiles of all mixed systems did not change significantly upon dilution with STF suggesting the maintenance of their pseudoplastic behavior (Fig. S4). Moreover, there was no marked change in the absolute values of η^* upon dilution except, again, in the case of PL2 sample.

Comparing our mixed P407/P188/CS systems with mixed P407/CS system developed by Gratieri et al.¹⁹ in terms of resistance to dilution, it may be concluded that P188 significantly contributed to gel stability. In mixed P407/CS system the concentration of P407 was higher (16%, w/w and 14%, w/w, upon dilution with STF) than in case of mixed P407/P188/CS system (14.2%, w/w and 12.09%, w/w, upon dilution with STF). However, upon dilution mixed P407/CS system behaved as viscoelastic solution at 35°C and decreased frequencies while mixed P407/P188/CS system behaved as soft gel.

Based on minimal polymer content (P407, P188, and CS concentration of 14.2%, 1.7% and 0.25%, w/w, respectively), favorable rheological characteristics ($T_{gel} = 31.1^\circ\text{C}$, $\eta^* = 2.1\text{ Pa} \times \text{s}$) and *in vitro* resistance to tear dilution ($G' 212.4\text{ Pa}$ and 175.3 Pa before and after dilution, respectively), the PL1 was selected as optimal *in situ* forming gel.

Effect of Active Pharmaceutical Ingredients on Temperature of Gelation and Complex Viscosity

The addition of APIs in the mixed P407/P188/CS system is expected to cause a modification of the physicochemical properties of *in situ* forming gels. Four ophthalmic APIs were selected in order to gain understanding of their effects on T_{gel} and η^* of selected PL1 *in situ* forming gel. We tested APIs in the concentrations and combinations relevant for topical ophthalmic use. API-loaded P407/P188/CS systems were characterized for T_{gel} and η^* before and after dilution with STF (Table 3). All APIs, except TOBRA, notably decreased T_{gel} in comparison with T_{gel} of PL1. This effect was highest for DEX showing the decrease of the T_{gel} for 8.5°C. DEX has already been shown to decrease the T_{gel} of P407-based *in situ* forming gels.^{33,34} Such an effect can be ascribed to the promotion of P407 self-assembly in the presence of hydrophobic drug allowing the formation of gel at lower temperatures.³⁵ The T_{gel} of the mixed P407/P188 systems was also reported to be affected by the addition

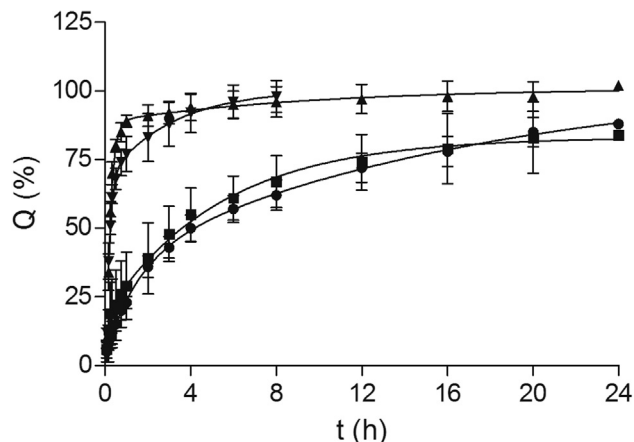


Figure 3. Release profiles of TIMO from PL1 (circles) and control *in situ* forming gel C1 (squares) with η^* comparable to PL1, control *in situ* forming gel C2 (triangle) with T_{gel} comparable to PL1 and TIMO solution (inverse triangle). The data are expressed as the mean \pm SD ($n = 5$).

of hydrophobic APIs; the T_{gel} decreased with increasing the pH-dependent hydrophobicity of API in the systems.³⁶ Smaller T_{gel} decrease was observed for the systems containing dissolved APIs, namely T_{gel} decreased for 4.8°C and 2.4°C in case of TIMO and DORZA, respectively. As anticipated by many authors, the decrease of T_{gel} induced by dissolved APIs could be related to the API salting-out effect.^{37,38} Their presence could shift the concentration and temperature at which micelles are formed to lower values and, moreover, could affect the close packing of micelles, resulting in T_{gel} decrease.^{32,36} However, despite the decrease of T_{gel} by the addition of APIs, all the samples except those with DEX formed gels at temperature higher than 25°C. The addition of APIs in the mixed P407/P188/CS system prolonged the gelation time in all cases except for DEX/TOBRA. However, the obtained gelation time values were still in the appropriate range (41.1-87.4 s) for ocular administration.^{39,40}

The η^* values for API-loaded PL1 were in the range of 1.52-7.88 Pa \times s indicating no pronounced influence of API entrapment on gel viscosity (Table 3).

Dilution with STF, as expected, led to the increase in T_{gel} and certain decrease in η^* for all the API-loaded PL1. All the samples retained their gel structure after dilution as suggested by the frequency sweep analysis (data not shown).

These results indicate the robustness of selected PL1 *in situ* forming gel against entrapment of APIs with different physicochemical characteristics. The decrease in T_{gel} caused by API entrapment open the possibility to further decrease the concentration of poloxamers required to obtain *in situ* forming gels with appropriate biopharmaceutical properties.⁴¹

Drug Release From In Situ Forming Gel

IVR study was performed to investigate the influence of viscosity related to the functional excipient concentration on the drug release rate. The optimal *in situ* forming gel (PL1) was characterized in terms of its influence on drug release profile. For that purpose, TIMO was selected as the model drug and incorporated in PL1 in the lowest efficient dose. Control *in situ* forming gel C1 was characterized by η^* comparable to PL1, whereas control *in situ* forming gel C2 was characterized by T_{gel} comparable to PL1 (Table 4). TIMO solution was also used as the control sample. The IVR profiles of PL1 and respective controls are shown in Figure 3. IVR of TIMO from PL1 and C1 was significantly slower than C2 and TIMO solution

indicating viscosity as the critical factor influencing drug release. Similar observations were already reported for *in situ* forming ophthalmic gels.^{26,42}

Biocompatibility Assessment of In Situ Forming Ophthalmic Gel

Biocompatibility of the optimal *in situ* forming gel (PL1) was assessed by using 2 3D cell-based corneal epithelial models, namely multilayered HCE-T epithelium cultivated on filters with 0.4 μ m pores and model consisting of an apical lipophilic HCE-T epithelial monolayer and a basolateral lipophilic monolayer of migrated HCE-T cell cultivated on filters with 3 μ m pores.⁴³ In the preliminary studies, simple 2D HCE-T monolayer was used to assess the formulation biocompatibility. However, exaggerated toxicity was found in comparison to *in vivo* studies.⁴⁴ *In vitro* 2D models are generally characterized by certain shortcomings, such as a more pronounced susceptibility to cytotoxicity, as they replicate only a limited segment of tissue structure/function.⁴⁵ Consequently, the concentration of polymers/formulation that can be safely applied to such models may be reduced in comparison to the *in vivo* system. Therefore, we employed more complex 3D corneal epithelial models to screen the formulation biocompatibility. Contrary to HCE-T epithelial monolayer, 3D models revealed biocompatibility of the formulation tested. Namely, 30-min treatment resulted in decrease in 3D model cell viability lower than 20%.

Conclusions

In this study, we developed *in situ* forming gel characterized by T_{gel} in physiologically relevant range, pseudoplastic behavior and resistance to dilution. D-optimal design was successfully applied to reduce the total polymer content in *in situ* forming P407/P188/CS gel while retaining its advantageous rheological properties. The developed system was proved to be robust against entrapment of APIs making it a suitable platform for ophthalmic delivery of active pharmaceutical ingredients with diverse physicochemical properties. Moreover, the developed *in situ* forming ophthalmic gel was proved to provide prolonged drug release in relation to the system viscosity.

ACKNOWLEDGMENTS

This work was supported by a Partnership in Research project 04.01/56 funded by the Croatian Science Foundation and PLIVA Croatia LTD.

References

1. Pepic I, Lovric J, Cetina-Cizmek B, Reichl S, Filipovic-Grcic J. Toward the practical implementation of eye-related bioavailability prediction models. *Drug Discov Today*. 2014;19(1):31-44.
2. Kirchof S, Goepferich AM, Brandl FP. Hydrogels in ophthalmic applications. *Eur J Pharm Biopharm*. 2015;95(Pt B):227-238.
3. Almeida H, Amaral MH, Lobao P, Lobo JM. In situ gelling systems: a strategy to improve the bioavailability of ophthalmic pharmaceutical formulations. *Drug Discov Today*. 2014;19(4):400-412.
4. Zignani M, Tabatabay C, Gurny R. Topical semisolid drug-delivery - kinetics and tolerance of ophthalmic hydrogels. *Adv Drug Deliv Rev*. 1995;16(1):51-60.
5. Destruel PL, Zeng N, Maury M, Mignet N, Boudy V. In vitro and in vivo evaluation of in situ gelling systems for sustained topical ophthalmic delivery: state of the art and beyond. *Drug Discov Today*. 2017;22(4):638-651.
6. El-Kamel AH. In vitro and in vivo evaluation of Pluronic F127-based ocular delivery system for timolol maleate. *Int J Pharm*. 2002;241(1):47-55.
7. Rupenthal ID, Green CR, Alany RG. Comparison of ion-activated in situ gelling systems for ocular drug delivery. Part 2: precorneal retention and in vivo pharmacodynamic study. *Int J Pharm*. 2011;411(1-2):78-85.
8. Almeida H, Amaral MH, Lobao P, Sousa Lobo JM. Applications of poloxamers in ophthalmic pharmaceutical formulations: an overview. *Expert Opin Drug Deliv*. 2013;10(9):1223-1237.

9. Trong LCP, Djabourov M, Ponton A. Mechanisms of micellization and rheology of PEO-PPO-PEO triblock copolymers with various architectures. *J Colloid Interf Sci.* 2008;328(2):278-287.
10. Wei G, Xu H, Ding PT, Li SM, Zheng JM. Thermosetting gels with modulated gelation temperature for ophthalmic use: the rheological and gamma scintigraphic studies. *J Control Release.* 2002;83(1):65-74.
11. Zhang M, Djabourov M, Bourgaux C, Bouchemal K. Nanostructured fluids from pluronic(R) mixtures. *Int J Pharm.* 2013;454(2):599-610.
12. Qi H, Li L, Huang C, Li W, Wu C. Optimization and physicochemical characterization of thermosensitive poloxamer gel containing puerarin for ophthalmic use. *Chem Pharm Bull (Tokyo).* 2006;54(11):1500-1507.
13. Kim EY, Gao ZG, Park JS, Li H, Han K. rhEGF/HP-beta-CD complex in poloxamer gel for ophthalmic delivery. *Int J Pharm.* 2002;233(1-2):159-167.
14. Asasutjarit R, Thanasanchokepibull S, Fuongfuchat A, Veeranondha S. Optimization and evaluation of thermoresponsive diclofenac sodium ophthalmic in situ gels. *Int J Pharm.* 2011;411(1-2):128-135.
15. Qi H, Chen W, Huang C, et al. Development of a poloxamer analogs/carbopol-based in situ gelling and mucoadhesive ophthalmic delivery system for puerarin. *Int J Pharm.* 2007;337(1-2):178-187.
16. Shastri DH, Prajapati ST, Patel LD. Thermoreversible mucoadhesive ophthalmic in situ hydrogel: design and optimization using a combination of polymers. *Acta Pharm.* 2010;60(3):349-360.
17. Mayol L, Quaglia F, Borzacchiello A, Ambrosio L, La Rotonda MI. A novel poloxamers/hyaluronic acid in situ forming hydrogel for drug delivery: rheological, mucoadhesive and in vitro release properties. *Eur J Pharm Biopharm.* 2008;70(1):199-206.
18. Lin HR, Sung KC, Vong WJ. In situ gelling of alginate/pluronic solutions for ophthalmic delivery of pilocarpine. *Biomacromolecules.* 2004;5(6):2358-2365.
19. Gratieri T, Gelfuso GM, Rocha EM, Sarmiento VH, de Freitas O, Lopez RF. A poloxamer/chitosan in situ forming gel with prolonged retention time for ocular delivery. *Eur J Pharm Biopharm.* 2010;75(2):186-193.
20. Basaran E, Yazan Y. Ocular application of chitosan. *Expert Opin Drug Deliv.* 2012;9(6):701-712.
21. de la Fuente M, Ravina M, Paolicelli P, Sanchez A, Seijo B, Alonso MJ. Chitosan-based nanostructures: a delivery platform for ocular therapeutics. *Adv Drug Deliv Rev.* 2010;62(1):100-117.
22. Tsai CY, Woung LC, Yen JC, et al. Thermosensitive chitosan-based hydrogels for sustained release of ferulic acid on corneal wound healing. *Carbohydr Polym.* 2016;135:308-315.
23. Paulsson M, Hagerstrom H, Edsman K. Rheological studies of the gelation of deacetylated gellan gum (Gelrite) in physiological conditions. *Eur J Pharm Sci.* 1999;9(1):99-105.
24. Schmolka IR. Artificial skin. I. Preparation and properties of pluronic F-127 gels for treatment of burns. *J Biomed Mater Res.* 1972;6(6):571-582.
25. Ammar HO, Salama HA, Ghorab M, Mahmoud AA. Development of dorzolamide hydrochloride in situ gel nanoemulsion for ocular delivery. *Drug Dev Ind Pharm.* 2010;36(11):1330-1339.
26. Gratieri T, Gelfuso GM, de Freitas O, Rocha EM, Lopez RF. Enhancing and sustaining the topical ocular delivery of fluconazole using chitosan solution and poloxamer/chitosan in situ forming gel. *Eur J Pharm Biopharm.* 2011;79(2):320-327.
27. Mezger TG. *The Rheology Handbook.* 4th ed. Hannover, Germany: Vincentz Network; 2014.
28. Pauly A, Meloni M, Brignole-Baudouin F, Warnet JM, Baudouin C. Multiple endpoint analysis of the 3D-reconstituted corneal epithelium after treatment with benzalkonium chloride: early detection of toxic damage. *Invest Ophthalmol Vis Sci.* 2009;50(4):1644-1652.
29. Bodea A, Leucuta SE. Optimization of hydrophilic matrix tablets using a D-optimal design. *Int J Pharm.* 1997;153(2):247-255.
30. Gupta H, Jain S, Mathur R, Mishra P, Mishra AK, Velpandian T. Sustained ocular drug delivery from a temperature and pH triggered novel in situ gel system. *Drug Deliv.* 2007;14(8):507-515.
31. Chaibundit C, Ricardo NM, Ricardo NM, et al. Aqueous gels of mixtures of ionic surfactant SDS with pluronic copolymers P123 or F127. *Langmuir.* 2009;25(24):13776-13783.
32. Aka-Any-Grah A, Bouchemal K, Koffi A, et al. Formulation of mucoadhesive vaginal hydrogels insensitive to dilution with vaginal fluids. *Eur J Pharm Biopharm.* 2010;76(2):296-303.
33. Arbelaez-Camargo D, Sune-Negre JM, Roig-Carreras M, et al. Preformulation and characterization of a lidocaine hydrochloride and dexamethasone sodium phosphate thermo-reversible and bioadhesive long-acting gel for intraperitoneal administration. *Int J Pharm.* 2016;498(1-2):142-152.
34. Meznarich NAK, Juggernaut KA, Batzli KM, Love BJ. Structural changes in PEO-PPO-PEO gels induced by methylparaben and dexamethasone observed using time-resolved SAXS. *Macromolecules.* 2011;44(19):7792-7798.
35. Sharma PK, Bhatia SR. Effect of anti-inflammatories on Pluronic F127: micellar assembly, gelation and partitioning. *Int J Pharm.* 2004;278(2):361-377.
36. Scherlund M, Brodin A, Malmsten M. Micellization and gelation in block copolymer systems containing local anesthetics. *Int J Pharm.* 2000;211(1-2):37-49.
37. Jeong B, Kim SW, Bae YH. Thermosensitive sol-gel reversible hydrogels. *Adv Drug Deliv Rev.* 2002;54(1):37-51.
38. van Hemelrijck C, Muller-Goymann CC. Rheological characterization and permeation behavior of poloxamer 407-based systems containing 5-aminolevulinic acid for potential application in photodynamic therapy. *Int J Pharm.* 2012;437(1-2):120-129.
39. Jaiswal M, Kumar M, Pathak K. Zero order delivery of itraconazole via polymeric micelles incorporated in situ ocular gel for the management of fungal keratitis. *Colloids Surf B Biointerfaces.* 2015;130:23-30.
40. Morsi N, Ghorab D, Refai H, Teba H. Ketorolac tromethamine loaded nano-dispersion incorporated into thermosensitive in situ gel for prolonged ocular delivery. *Int J Pharm.* 2016;506(1-2):57-67.
41. Sharma PK, Reilly MJ, Bhatia SK, Sakhitab N, Archambault JD, Bhatia SR. Effect of pharmaceuticals on thermoreversible gelation of PEO-PPO-PEO copolymers. *Colloids Surf B Biointerfaces.* 2008;63(2):229-235.
42. Rupenthal ID, Green CR, Alany RG. Comparison of ion-activated in situ gelling systems for ocular drug delivery. Part 1: physicochemical characterisation and in vitro release. *Int J Pharm.* 2011;411(1-2):69-77.
43. Juretic M, Jurisic Dukovski B, Krtalic I, et al. HCE-T cell-based permeability model: a well-maintained or a highly variable barrier phenotype? *Eur J Pharm Sci.* 2017;104:23-30.
44. Furrer P, Plazonnet B, Mayer JM, Gurny R. Application of in vivo confocal microscopy to the objective evaluation of ocular irritation induced by surfactants. *Int J Pharm.* 2000;207(1-2):89-98.
45. Fitzgerald KA, Malhotra M, Curtin CM, O'Brien FJ, O'Driscoll CM. Life in 3D is never flat: 3D models to optimise drug delivery. *J Control Release.* 2015;215:39-54.